Spectral tuning of a three-dimensional photonic-bandgap waveguide signature by silica atomic-layer deposition

Isabelle Staude,[1,*] **Georg von Freymann,**[1,2] **and Martin Wegener**[1,2]

[1]*Institut für Angewandte Physik and DFG-Center for Functional Nanostructures (CFN), Karlsruhe Institute of Technology (KIT), D-76131 Karlsruhe, Germany*
[2]*Institut für Nanotechnologie, Karlsruhe Institute of Technology (KIT), D-76021 Karlsruhe, Germany*
[*]*ips124@physics.anu.edu.au*

Abstract: Recent progress in three-dimensional sub-micron fabrication has rendered the introduction of waveguide structures into optical three-dimensional photonic bandgap materials possible. However, spectral tuning of the waveguide modes has not been demonstrated so far. Here, we use atomic-layer deposition of amorphous silica to tune the spectral position of an air-core defect waveguide in a three-dimensional silicon woodpile photonic crystal by 225 nm in wavelength. The measured spectral positions of the waveguide signature are in very good agreement with numerical calculations.

OCIS codes: (130.5296) Photonic crystal waveguides; (160.5293) Photonic bandgap materials.

References and links

1. M. Bayindir, E. Ozbay, B. Temelkuran, M. M. Sigalas, C. M. Soukoulis, R. Biswas, and K. M. Ho, "Guiding, bending, and splitting of electromagnetic waves in highly confined photonic crystal waveguides," Phys. Rev. B **63,** 081107 (2001).
2. M. L. Povinelli, S. G. Johnson, S. Fan, and J. D. Joannopoulos, "Emulation of two-dimensional photonic crystal defect modes in a photonic crystal with a three-dimensional photonic band gap," Phys. Rev. B **64,** 075313 (2001).
3. Z.-Y. Li and K. M. Ho, "Waveguides in three-dimensional layer-by-layer photonic crystals," J. Opt. Soc. Am. B **20,** 801–809 (2003).
4. A. Chutinan, S. John, and O. Toader, "Diffractionless Flow of Light in All-Optical Microchips," Phys. Rev. Lett. **90**, 123901 (2003).
5. A. Chutinan and S. John, "Light localization for broadband integrated optics in three dimensions," Phys. Rev. B **72,** 161316 (2005).
6. B. M. Cowan, "Three-dimensional dielectric photonic crystal structures for laser-driven acceleration," Phys. Rev. Spec. Top. Accel. Beams **11,** 011301 (2008).
7. I. Staude, C. McGuinness, A. Frölich, R. L. Byer, E. Colby, and M. Wegener, "Waveguides in three-dimensional photonic bandgap materials for particle-accelerator on a chip architectures," Opt. Express **20,** 5607–5612 (2012).
8. S. A. Rinne, F. García-Santamaría, and P. V. Braun, "Embedded cavities and waveguides in three-dimensional silicon photonic crystals," Nat. Photonics **2,** 52–56 (2008).
9. S. Kawashima, K. Ishizaki, and S. Noda, "Light propagation in three-dimensional photonic crystals," Opt. Express **18,** 386–392 (2010).
10. I. Staude, G. von Freymann, S. Essig, K. Busch, and M. Wegener, "Waveguides in three-dimensional photonic-band-gap materials by direct laser writing and silicon double inversion," Opt. Lett. **36,** 67–69 (2011).
11. A. Tandaechanurat, S. Ishida, K. Aoki, D. Guimard, M. Nomura, S. Iwamoto, and Y. Arakawa, "Demonstration of high-Q (>8600) three-dimensional photonic crystal nanocavity embedding quantum dots," Appl. Phys. Lett. **94,** 171115 (2009).

#162003 - $15.00 USD Received 25 Jan 2012; revised 15 Mar 2012; accepted 6 Apr 2012; published 11 Apr 2012

12. G. Subramania, Y.-J. Lee, and A. J. Fischer, "Silicon-Based Near-Visible Logpile Photonic Crystal," Adv. Mater. **22,** 4180–4185 (2010).
13. G. Subramania, Q. Li, Y.-J. Lee, J. J. Figiel, G. T. Wang, and A. J. Fischer, "Gallium Nitride Based Logpile Photonic Crystals," Nano Lett. **11,** 4591–4596 (2011).
14. N. Tétreault, G. von Freymann, M. Deubel, M. Hermatschweiler, F. Pérez-Willard, S. John, M. Wegener, and G. A. Ozin, "New Route to Three-Dimensional Photonic Bandgap Materials: Silicon Double Inversion of Polymer Templates," Adv. Mater. **18,** 457–460 (2006).
15. C. J. Chen, C. A. Husko, I. Meric, K. L. Shepard, C. W. Wong, W. M. J. Green, Y. A. Vlasov, and S. Assefa, "Deterministic tuning of slow-light in photonic-crystal waveguides through the C and L bands by atomic layer deposition," Appl. Phys. Lett. **96,** 081107 (2010).
16. S. Kiravittaya, H. S. Lee, L. Balet, L. H. Li, M. Francardi, A. Gerardino, A. Fiore, A. Rastelli, and O. G. Schmidt, "Tuning optical modes in slab photonic crystal by atomic layer deposition and laser-assisted oxidation," Adv. Mater. **109,** 053115 (2011).
17. Y. Lin and P. R. Herman, "Effect of structural variation on the photonic band gap in woodpile photonic crystal with body-centered-cubic symmetry," J. Appl. Phys. **98,** 063104 (2005).
18. I. Staude, M. Thiel, S. Essig, C. Wolff, K. Busch, G. von Freymann, and M. Wegener, "Fabrication and characterization of silicon woodpile photonic crystals with a complete bandgap at telecom wavelengths," Opt. Lett. **35,** 1094–1096 (2010).
19. D. J. Ehrlich and J. Melngailis, "Fast room-temperature growth of SiO2 films by molecular-layer dosing," Appl. Phys. Lett. **58,** 2675–2677 (1991).
20. S. G. Johnson and J. D. Joannopoulos, "Block-iterative frequency-domain methods for Maxwell's equations in a planewave basis," Opt. Express **8,** 173–190 (2001).
21. A. Frölich and M. Wegener, "Spectroscopic characterization of highly doped ZnO films grown by atomic-layer deposition for three-dimensional infrared metamaterials," Opt. Mater. Express **1,** 883–889 (2011).

1. Introduction

While two-dimensional photonic crystals and defects/waveguides therein have already found several applications, *e.g.*, in forming high-quality optical cavities, for slow light, or for coupling light out of light-emitting diodes, the fabrication of three-dimensional (3D) photonic-bandgap (PBG) materials remains challenging. Accordingly, there is still some way to go regarding their unique potential applications, like, most prominently, ultra-compact all-optical three-dimensional photonic circuitry [1–5], or less obviously, accelerating segments for particle-accelerator-on-a-chip architectures. Corresponding accelerator structures have recently been proposed on the basis of air-core waveguides in a silicon-woodpile 3D PBG material [6]. First steps towards their experimental realization have been demonstrated [7].

Despite the huge challenge to actually fabricate corresponding waveguide structures for operation wavelengths in the optical regime, light propagation through 3D PBG waveguides has recently been reported by several groups [8–10]. The realization of cavities and planar defect structures has, e.g., been demonstrated in [11–13]. However, due to fabrication inaccuracies, target operation wavelengths of the designed waveguide structures can often not be met exactly. This failure to meet a target wavelength becomes critical when the operation wavelength is externally fixed, *e.g.*, by the exciting laser source, or if several 3D PBG-material based devices with slightly different mode frequencies have to be adjusted to operate at the same frequency. For example, in Ref. [6] several photonic particle-accelerator segments are supposed to be excited by the same laser source, such that all these elements have to operate at exactly the same wavelength. Hence, a precise tuning method is very strongly desired.

To overcome this problem, we here suggest and demonstrate an ex-post tuning method to experimentally shift the spectral position of the 3D PBG waveguide mode of an already fabricated structure to a desired position. This method relies on atomic layer deposition (ALD) to infiltrate the waveguide structures with thin layers of dielectric. While ALD has previously been used to adjust geometric parameters of bulk photonic crystals [14] and to tune optical modes in two-dimensional photonic crystal slabs [15, 16], this is the first time it is successfully employed to induce systematic changes in the optical properties of a 3D PBG waveguide. In

#162003 - $15.00 USD Received 25 Jan 2012; revised 15 Mar 2012; accepted 6 Apr 2012; published 11 Apr 2012

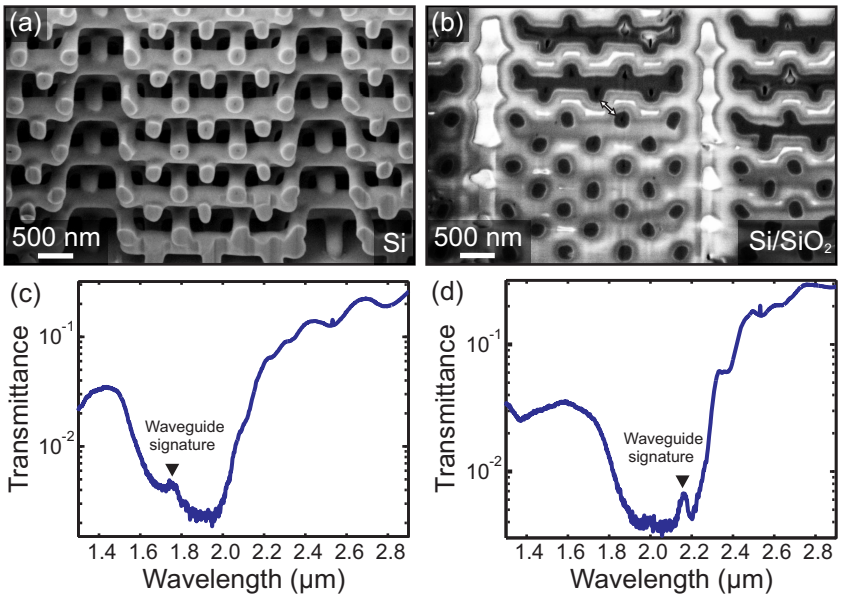

Fig. 1. (a) Oblique-view electron micrograph of a FIB cross-section revealing two vertical waveguides within the silicon woodpile structure. (b) The same structure after complete infiltration by silica ALD. Silicon appears in dark gray, silica in light gray. White regions stem from electric charging effects. The arrow marks the position of the infiltration bottleneck in the woodpile structure. Note that the FIB cut plane and the corresponding woodpile lattice plane are slightly tilted with respect to each other. (c) Linear-optical transmittance spectrum for the woodpile waveguide structure before infiltration (data taken from Ref. [10]), and (d) for the completely silica filled structure.

principle the method is not limited to the waveguides considered here but it can be applied to any 3D photonic crystal defect structure suitable for infiltration, including point-defect cavities. However, in order to achieve substantial spectral tuning of the waveguide mode while at the same time changing the properties of the host PBG material to a much lesser degree, the waveguide has to be designed such that it concentrates a significant part of the mode energy inside air and in close vicinity to an air-material interface. This is, in particular, not the case for dielectric defects where the mode energy is predominantly concentrated in the high-index dielectric and only minor spectral defect mode shifts can be expected by infiltration.

2. Experimental

The starting point for our present work is a body-centered cubic silicon woodpile structure [17] containing a two-dimensional array of straight vertical air-core waveguides arranged on a 4×4 super cell as described in our previous work [10]. The structure has been fabricated using a combination of direct laser writing and silicon double inversion [14, 18]. An electron micrograph of the structure is shown in Fig. 1(a). In this image, focused-ion-beam (FIB) milling has been performed to reveal two of the waveguides inside the woodpile structure. The overall footprint of the woodpile is $40\,\mu\text{m} \times 40\,\mu\text{m}$. Numerical calculations performed for an ideal structure with experimental woodpile parameters suggest the existence of a 3D PBG with 15.4% gap-midgap ratio in this structure [10]. Additional calculations reveal that the waveguide supports a two-fold degenerate mode inside the 3D PBG around $1.75\,\mu\text{m}$ wavelength [10]. In experimental spectra

#162003 - $15.00 USD Received 25 Jan 2012; revised 15 Mar 2012; accepted 6 Apr 2012; published 11 Apr 2012

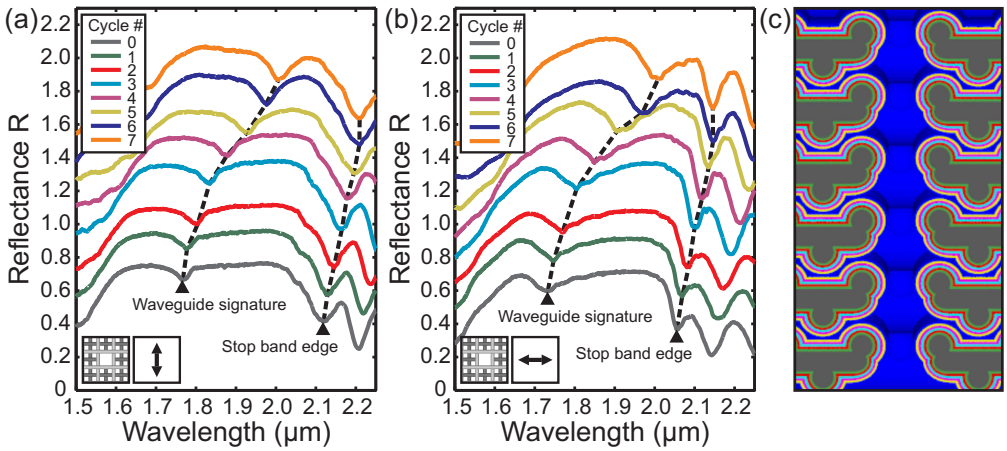

Fig. 2. (a), (b) Linear-optical reflectance spectra of the waveguide-containing silicon woodpile structure for linearly polarized incident light, measured after subsequent individual cycles of silica ALD. Spectra for subsequent cycles are offset by $R = 0.2$. The black dashed lines are guides to the eye, highlighting the respective experimental positions of the waveguide mode signature and the dielectric stop band edge. The insets indicate the respective directions in which the electric field of the linearly polarized incident light is oriented with respect to the topmost woodpile layer. (c) Visualization of the ideal woodpile waveguide structure after 6 cycles of silica ALD. Silicon is depicted in dark gray. The colors assigned to the different silica layers aim to connect this image to the experimental spectra shown in (a) and (b).

this mode appears as a narrow peak in transmittance and dip in reflectance located inside the photonic stop band in spectroscopy direction [10].

In order to tune the spectral position of this waveguide signature the waveguide-containing 3D PBG material has been infiltrated stepwise by several individual cycles of silica atomic-layer deposition (ALD) [19]. Silica has been chosen for three reasons: First, the silica deposition process is performed at room temperature and under ambient pressure, which results in a gentle treatment of the infiltrated sample. Second, its relatively low refractive index allows for small and precise adjustments of the waveguide mode frequency. Third, silica can be etched out of the silicon PBG material selectively, thereby offering the opportunity of re-using samples several times. For silica deposition we use silicon tetrachloride ($SiCl_4$) and water (H_2O) as precursors and nitrogen as carrier gas. Every ALD cycle consists of a 5 min pulse of H_2O and a 1.5 min pulse of $SiCl_4$. Between subsequent pulses we have allowed for a purge period of 5 min. After each cycle approximately 25 nm of silica are deposited at all accessible air-material interfaces inside the 3D structure. An oblique-view electron micrograph of a FIB cross-section of the completely infiltrated structure after the initial 7 cycles plus 5 additional cycles of ALD is displayed in Fig. 1(b). After each ALD cycle, reflectance spectra of the sample are taken using a commercial Fourier-transform microscope-spectrometer (Bruker, Equinox 55, Opticon 36× Cassegrain objective). As the degeneracy of the waveguide mode is lifted due to sample imperfections we use linearly polarized light in these measurements in order to obtain clear waveguide signatures. While these measurements can in principle also be performed in transmittance mode, the waveguide signature appears more pronounced in reflectance, where the signal intensity level is far away from the measurement limit of the instrument. In order to provide additional evidence of the actual waveguiding functionality of our structures linear-optical transmittance spectra for unpolarized incident light are displayed in Figs. 1(c) and 1(d). In Fig. 1(c) transmittance is

#162003 - $15.00 USD Received 25 Jan 2012; revised 15 Mar 2012; accepted 6 Apr 2012; published 11 Apr 2012

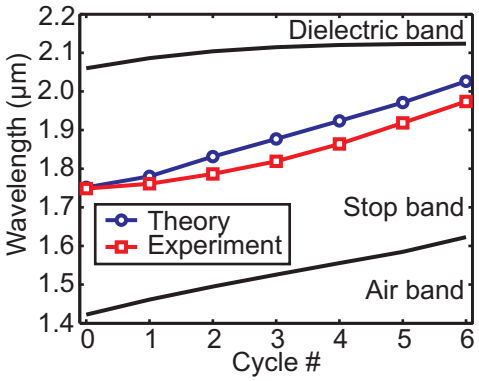

Fig. 3. Calculated mid-band position of the degenerate waveguide mode (blue) and measured polarization-averaged waveguide signature positions found in the experiment (red) after each silica ALD cycle. After 6 cycles the host woodpile structure is completely infiltrated.

plotted for the un-infiltrated silicon structure [10], Fig. 1(d) shows transmittance through the silica-silicon composite structure measured before initial silica removal, which is nominally identical to the completely infiltrated case. In both cases the waveguide mode appears as a distinct peak inside the photonic stop band, clearly demonstrating that light is indeed propagating through the waveguides.

3. Results and discussion

The results of our reflectance measurements performed after each ALD cycle are depicted in Figs. 2(a) and 2(b). An example cross-section image of the ideal infiltrated structure is shown in Fig. 2(c). For both polarizations, the waveguide mode successively shifts towards longer wavelengths after each cycle owing to the increase of silica-layer thickness in the defect channel. The entire stop band also shifts red, but in smaller steps. From cycle 6 to cycle 7, no further shift of the stop band can be observed any more, indicating that the host woodpile structure is completely infiltrated after completion of cycle 6. At this point the silica layer has reached a thickness of half the infiltration bottleneck of the woodpile structure. Thus, the precursor gases can no longer penetrate into the 3D structure any more and material deposition inside stops. The bottleneck appears between neighboring rods in next but one layers, as highlighted by the arrow in Fig. 1(b). Using the same structure parameters as in Ref. [10] (lateral rod distance $a = 782\,\mathrm{nm}$, lateral rod diameter $d = 0.28 \times a$, rod aspect ratio $\chi = 1.3$, vertical stacking period $c = a$), the bottleneck width is calculated to be 303 nm, resulting in a maximum silica layer thickness of 151.5 nm that can be deposited in the woodpile structure before the bottlenecks are closed.

The waveguide channel, on the other hand, is not yet completely infiltrated after deposition of 151.5 nm of silica and the precursor gases responsible for silica growth can still penetrate this region from the top of the sample. This can also be observed from Fig. 1(b), where the silica layer thickness deposited in the defect region is obviously larger than in the surrounding woodpile material. Consequently, while the stop band position remains unchanged after cycle 6, the waveguide mode is further red-shifted by the 7th ALD cycle. In order to compare these experimental findings with theory, numerical band-structure calculations that include the respective silica layer thickness have been performed for each ALD cycle contributing to the complete infiltration of the host woodpile structure, namely for cycles 1 to 6. For these calculations we have

#162003 - $15.00 USD Received 25 Jan 2012; revised 15 Mar 2012; accepted 6 Apr 2012; published 11 Apr 2012

used the freely available MIT-Photonic-Bands (MPB) package [20]. In accordance with the experiment a 4×4 computational super cell is used. The silica layer thickness deposited at each ALD cycle is set to one sixth of the theoretical half-width of the bottleneck, that is 25 nm. The refractive index of the silica is taken as 1.45 and for the uninfiltrated structure we have again used the same structure parameters as in Ref. [10] and as visualized in Fig. 2(c) (woodpile structure parameters as above, length of missing rod section $L = 0.73 \times a$, effective value of the silicon dielectric constant $\varepsilon = 11$). Corresponding calculation results are shown in Fig. 3, where the mid-band positions (blue) of the waveguide mode are plotted over the performed number of ALD deposition cycles. The calculated mid-band position is shifted by 279 nm from 1.752 μm for the uninfiltrated case to 2.031 μm for the completely infiltrated structure, while the shift found for the dielectric band edge (63 nm from 2.060 μm to 2.123 μm) is significantly smaller. This is in good qualitative agreement with experimental observations for the waveguide signature position (red line) also included in Fig. 3. The plotted experimental data correspond to the dip minima positions averaged over the two measured linear polarizations. Quantitatively, the shift is slightly smaller in the experiment compared to theory, namely 225 nm from 1.749 μm to 1.974 μm, which can be attributed to deviations from perfect periodicity narrowing down the effective width of the bottlenecks. This results in an overestimate of the actually deposited silica-layer thickness and, thus, in an overestimated shift. It is worth mentioning that not only the mid-band position, but also the expected bandwidth of the waveguide mode is changed by silica infiltration. Starting from cycle 2, it is continuously increased towards larger cycle numbers from 9 nm after cycle 2 to 59 nm after cycle 6. Qualitatively, this behavior can also be found in the experiment, where the dips become broader and more pronounced as the number of performed ALD cycles increases (see Figs. 2(a) and 2(b)). We refrain from a quantitative analysis here as our measurement averages over approximately 20 individual waveguides in the measurement region, thereby leading to an inhomogeneous-broadening effect.

It should be clear that infiltration of the entire woodpile structure with silica does not only affect the waveguide mode properties, but also those of the bulk structure. In particular, the size of the PBG is decreased by the reduction of the refractive-index contrast. After one ALD cycle, the above calculations still predict a complete 3D PBG with a gap-midgap ratio of 14.4%; for the completely infiltrated structure this value is reduced to 0.7%. Nevertheless, while we have intentionally deposited relatively thick films (25 nm) in this work in order to create substantial wavelength shifts of the waveguide signature for the purpose of clear demonstration, a very precise fine-tuning can also easily be achieved using this method, as ALD allows for monolayer material deposition. In this case, *i.e.*, if only very thin layers of silica or other dielectric materials amenable to ALD are infiltrated into the woodpile structure, the size of the PBG is only marginally decreased. Apart from varing the spaial distribution of the real part of the dielectric function by infiltration one could also imagine varying its imaginary part by ALD of a lossy material, *e.g.*, doped ZnO [21], which could be employed for selective mode damping.

4. Conclusion

In conclusion, we have experimentally demonstrated spectral tuning of a 3D PBG waveguide mode by cycle-wise infiltration of the waveguide containing silicon woodpile structure via silica ALD. Tuning over a wavelength range of approximately 225 nm or 13% has been achieved. These results are in good agreement with corresponding band-structure calculations.

Acknowledgments

We acknowledge support by the Deutsche Forschungsgemeinschaft (DFG) and the State of Baden-Württemberg through the DFG-Center for Functional Nanostructures (CFN) within subproject A 1.4. The research of G.v.F. is further supported through a DFG Emmy-Noether fel-

lowship (DFG-FR 1671/4-3). We acknowledge support by Deutsche Forschungsgemeinschaft and Open Access Publishing Fund of Karlsruhe Institute of Technology.

#162003 - $15.00 USD Received 25 Jan 2012; revised 15 Mar 2012; accepted 6 Apr 2012; published 11 Apr 2012